CNS Neuroscience & Therapeutics

ORIGINAL ARTICLE

CNS Neuroscience & Therapeutics

MiR-150 Regulates Poststroke Cerebral Angiogenesis via Vascular Endothelial Growth Factor in Rats

Quan-Wei He, Qian Li, Hui-Juan Jin, Fang Zhi, Baral Suraj, Yi-Yi Zhu, Yuan-Peng Xia, Ling Mao, Xiao-Lu Chen & Bo Hu

Department of Neurology, Union Hospital, Tongji Medical College, Huazhong University of Science and Technology, Wuhan 430022, China

Keywords
Angiogenesis; Brain microvascular endothelial cells; miR-150; Stroke; Vascular endothelial growth factor.

Correspondence
Bo Hu, Ph.D. M.D., Department of Neurology, Union Hospital, Tongji Medical College, Huazhong University of Science and Technology, Wuhan 430022, China.
Tel.: +86-13-707114863;
Fax: +86-27-85726028;
E-mail: hubo@mail.hust.edu.cn
Received 10 November 2015; revision 20 January 2016; accepted 24 January 2016

doi: 10.1111/cns.12525

SUMMARY

Aims: Angiogenesis is a harmonized target for poststroke recovery. Therefore, exploring the mechanisms involved in angiogenesis after stroke is vitally significant. In this study, we are reporting a miR-150-based mechanism underlying cerebral poststroke angiogenesis. **Methods:** Rat models of middle cerebral artery occlusion (MCAO) and cell models of oxygen–glucose deprivation were conducted. Capillary density, tube formation, cell proliferation, and cell migration were measured by FITC-dextran assay, matrigel assay, Ki-67 staining, and wound healing assay, respectively. The expression of miR-150 and vascular endothelial growth factor (VEGF) was, respectively, measured by RT-PCR and Western blotting. Dual-luciferase assay was conducted to confirm the binding sites between miR-150 and VEGF. **Results:** We found that miR-150 expression in the brain and serum of rats subjected to cerebral ischemia, and in oxygen–glucose-deprived brain microvascular endothelial cells (BMVECs) and astrocytes. Upregulation of miR-150 expression could decrease vascular density of infarct border zone in rat after MCAO and decrease tube formation, proliferation, and migration of BMVECs. We also found that miR-150 could negatively regulate the expression of VEGF, and VEGF was confirmed to be a direct target of miR-150. Moreover, VEGF mediated the function of miR-150 on tube formation, proliferation, and migration of BMVECs. **Conclusions:** Our data suggested that miR-150 could regulate cerebral poststroke angiogenesis in rats through VEGF.

Introduction

Induction of angiogenesis is one of the most promising therapeutic strategies for stroke and it helps to restore blood supply after the attack, thereby promoting recovery of brain function [1, 2]. Following stroke, angiogenic factors of various sorts may be activated to overcome hypoxia to restore oxygen and nutrient homeostasis. Among these angiogenic growth factors, vascular endothelial growth factor (VEGF) has been demonstrated to be one of the major contributors to poststroke neovascularization [3]. But the effect of post-transcriptional regulation of VEGF in brain microvascular endothelial cells (BMVECs) on angiogenesis has remained largely unexplored, thus requiring much more effort to understand the molecular mechanism that regulates angiogenesis.

Over the past years, our research effort has been directed at poststroke angiogenesis and we found that sonic hedgehog (SHH) could promote angiogenesis via VEGF after oxygen–glucose deprivation or stroke [4–6]. However, SHH, as an angiogenic factor, does not work directly on VEGF, a key angiogenic regulator [7], and the regulation of poststroke VEGF expression remains further research. Ghorpade et al. [8] reported that SHH can induce miR-31 and miR-150 after mycobacterium bovis infection. Thus, we noticed miRNAs and speculated that miR-150 might be a pivotal epigenetic regulator of VEGF.

miR-150 is a relatively evolutionarily conserved microRNA in mammals and was found that played an important role in the hematopoiesis [9] and tumorigenesis [10–12] in previous studies. However, it was also reported recently that miR-150 might be an important microRNA regulating angiogenesis. MiR-150 was implicated in the differentiation of human endothelial lineage and vasculogenesis of chick embryos [13]. MiR-150 was also crucial for retinal angiogenesis [14], and macrophage-derived microvesicles induced angiogenesis and tumorigenesis [15]. Moreover, miR-150 can suppress pathologic ocular neovascularization [16]. All these studies suggested that miR-150 might regulate neovascularization via various targets under different pathophysiological conditions. Nonetheless, the role of miR-150 in angiogenesis after stroke has been poorly studied.

In this study, we found that miR-150, responsive to oxygen–glucose deprivation (OGD)/stroke, could mediate poststroke angiogenesis via VEGF.

Materials and Methods

The Animal Care and Use Committee (ACUC) of Huazhong University of Science and Technology (HUST) approves all the animal protocols and procedures.

MCAO Model Establishment

This mode was prepared according to our previous report [17]. Sprague Dawley rats, male, weighing 280–320 g, 8–9 weeks old, were used, which were obtained from and maintained in the ACUC of HUST. Briefly, rats were divided into different groups randomly and then anesthetized intraperitoneally with 40 mg/kg pentobarbital. After a midline incision, right common carotid artery (CCA), internal carotid artery (ICA), and external carotid artery (ECA) were isolated, and then, the right ECA was ligated. Then, a 4-0 poly-L-lysine-coated nylon suture (Sunbio Biotech Co Ltd, Beijing, China) was inserted from right ECA into the right ICA and then forwarded for 18 mm to the origin of middle cerebral artery (MCA). Rectal temperature was maintained at 37.3 ± 0.5°C during the procedures. Neurobehavioral functions test and brain perfusion by laser-Doppler flowmetry were used to confirm the success of surgery. Sham-operated group without the filament insertion were carried out with identical procedures.

Serum and Brain Sampling

Rats were anesthetized and sacrificed, and the blood and brain samples were obtained immediately after 1, 3, and 7 days of MCAO. Two-microliters of blood was obtained immediately at each time point, coagulated for 30 min, and then isolated the serum. The brain samples were obtained from the IBZ and divided equally immediately. The serum and brain samples were frozen at −20 °C as soon as possible, and for longtime storage were lastly transferred to −80°C.

Primary Culture of Rat Brain Microvascular Endothelial Cells

According to our published protocols [4], Sprague Dawley rats (n = 4, 40 g, 4 weeks of age) were used to isolate rat BMVECs. Briefly, rats were sterilized and sacrificed to collect the brains tissues, then leptomeninges, surface vessels, brain stem, and white matter were removed carefully, and so the cerebral cortices were isolated. After that, the cortices were put into preparatory ice-cold phosphate-buffered saline (PBS), cut into pieces immediately (about 1 mm^3), and then gently homogenized. The homogenized samples were then immediately centrifuged at 4°C (500 g × 10 min). Then, pellets were obtained and resuspended into 20% bovine serum albumin (BSA) and then centrifuged again at 4°C (1000 g × 20 min), and then, microvessels were found in the lower layer. Microvessels then were transferred into a new tube and washed with PBS. With 0.1% collagenase II/dispase plus DNase I (1000 IU/mL), the microvessels were digested at 37°C for 45 min. After that, the digested microvessels were centrifugation at 4°C (500 g × 10 min), the pellets were resuspended with 10 mL M131 medium (Invitrogen, Carlsbad, CA, USA) premixed with the microvascular growth supplement (Invitrogen) according to the commercial manual. Cell suspension was then seeded onto 6-cell plates, incubated in humidified air (5% CO_2, 95% O_2) at 37°C, and the 4th – 6th passages of purity exceeding 95% were used.

Primary Culture of Rat Astrocytes

To harvest rat astrocytes, newborn Sprague Dawley rats (n = 4) were used according to our published protocols [4]. Briefly, cerebral cortices were isolated, minced, and digested by 0.25 mg/mL trypsin and 0.1 mg/mL DNase at 37°C for 20 min. After centrifugation, the cells pellets were resuspended to high glucose Dulbecco's modified Eagle's medium (DMEM) supplemented with 10% fetal bovine serum (FBS), and then cells were seeded onto 6-cell plates, incubated, and maintained in humidified air (5% CO_2, 95% O_2) at 37°C. Fourteen days later, the plates were gently shaken (250 rpm × 18 h) to remove microglial cells and oligodendrocytes. The 4th – 6th passages of purity exceeding 95% were used.

micr*ON*® miRNA Agomir Intracerebroventricular Injection

Micr*ON*® miRNA agomir (RIBOBIO, Guangzhou, China), a specifically chemical modified microRNA agonist, has stable and long-lasting (up to 6 weeks) miRNA promotion effect. 5 μL of miR-150 agomir (1 nmol/L) or agomir control (1 nmol/L) was injected into right cerebral ventricle of rats (2.5 mm lateral from midline, 1.0 mm behind the bregma, and 3.0 mm deep from the skull surface). Agents were gently and slowly injected (1 μL/min), and to minimize back-flow, the micro-injector was maintained for 2 min before withdraw. The agents were administered 30 min before focal cerebral ischemia.

Oxygen–Glucose Deprivation

In accordance with a previous report with some modifications [4], in brief, cells were exposed to OGD for 2, 4 h, and then resumed with the oxygen and glucose supply for 24 h. To obtain OGD condition, the medium with no glucose (116 mM NaCl, 1.8 mM $CaCl_2$, 5.4 mM KCl, 0.8 mM $MgSO_4$, 1 mM NaH_2PO_4, 26.2 mM $NaHCO_3$, and 0.01 mM glycine) were pretreated with 95% N_2 and 5% CO_2 for 20 min, and cells were culture into the anaerobic incubator (95% N_2, 5% CO_2) at 37°C.

Down-modulation and Over-expression of miRNA

Brain microvascular endothelial cells were seeded onto 24-well plates for 24 h, and then, miR-150 inhibitor or miR-150 mimic was transfected into BMVECs by lipofectamine 2000 (RIBOBIO, Guangzhou, China) on the following day according to the commercial manual. Two solutions were prepared as follows: a mixture of 1 μL Lipofectamine2000 transfection agent in 50 μL Opti-MEM medium and a mixture of 2.5 μL miR-150 inhibitor or mimic or the corresponding negative control in 50 μL Opti-MEM medium per well. The two solutions were mixed for 30 min at 37°C, and miRNA reached a concentration of 100 nM. 100 μL combined mixture was added into each well with 400 μL culture medium. Cells were prepared for follow-up tests 24 h after transfection.

VEGF Neutralizing

To confirm the function of endogenous VEGF in miR-150-mediated angiogenesis *in vitro*, tube formation assay, proliferation assay, and wound healing assay in BMVECs were repeated with 0.5 μg/mL VEGF-neutralizing antibody (Abcam, Cambridge, MA, USA) pretreatment for 24 h according to manufacturer's instructions.

Observation of Tube Formation

Matrigel (BD Biosciences, San Jose, CA, USA) was thawed at 4°C, and 150 μL was used to coat each well of a 48-well plate. The plate was incubated at 37°C for 30 min to polymerize the Matrigel. BMVECs (5×10^4 cells/100 μL) were suspended in M131 containing microvascular growth supplement, plated into a Matrigel-coated well, and incubated at 37°C for 24 h. Tube length was quantitatively determined by ImageJ software package at ×40 magnifications from pictures captured. Each sample was examined in three randomly selected fields, and the examination was repeated three times.

Proliferation Assay

Cell proliferation was observed by immunofluorescent with a proliferation marker Ki-67 (rabbit anti-Ki-67; 1:100; Abcam) as mentioned previously [4]. Cells of Ki-67-positive staining were counted at ×200 magnifications from the pictures captured. Each sample was observed in three randomly chosen fields, and the observation was repeated three times.

Wound Healing Assay

As mentioned previously [4], 5×10^5 per well BMVECs were incubated for 24 h on 24-well plates for forming confluent monolayer, then, BMVECs were scratched with a 200-μL pipette tip, and then, suspension cells and the cell debris were cleared by three times wash with PBS. After cultured with fresh serum-free cell medium, BMVECs monolayer was allowed to heal for 24 h. Pictures were taken at the same place at 0 h and 24 h after injury. The healing of wounds was assessed with ImageJ software package by measuring the wound gap. The assay was repeated three times.

miRNA Real-time Quantitative PCR

Real-time fluorescence quantitative reverse-transcription PCR was used to evaluate miR-150 expression in BMVECs, astrocytes, rat brain, and blood samples. With Trizol Reagent (Invitrogen), total RNA was extracted from the samples, reversely transcribed with a miRNA cDNA Synthesis Kit (Takara Bio Inc, Shiga, Japan), and then amplified with a SYBR® Premix Ex TaqTM Kit (Takara Bio Inc). Primer sequences are forward 5′-TCTCCCAACCCTTGT ACCAGTG-3′ for miR-150, 5′-CTCGCTTCGGCAGCACA-3′ for U6, 5′-TAGCAGCACGTAAATATTGGCG-3′ for miR-16, while the common reverse primer sequence which provided by SYBR® Premix Ex TaqTM Kit was used for miR-150, U6, and miR-16 according to manufacturers' manual. Data were analyzed by the comparative CT method (2-ΔΔCT) and normalized to U6 for BMVECs and rat brain samples, and miR-16 for serum, miR-150 expression of brain samples, and serum in the IBZ were then normalized to the contralateral side. All the data of miRNA expression were showed as fold changes relative to the control group. All reactions were performed in triplicate.

Dual-luciferase Reporter Assay

To explore whether VEGF is the direct target of miR-150, dual-luciferase reporter assay were adopted. The 3′-untranscribed region (UTR) of rat VEGF mRNA containing the putative binding sites of miR-150 was generated and cloned into the pmiR-RB-REPORT TM luciferase reporter plasmid (Genechem, Shanghai, China). The dual-luciferase reporter plasmids, pmiR-VEGF-wt (containing the wild-type VEGF putative 3′-UTR binding site) and pmiR-VEGF-mut (containing the mutant VEGF 3′-UTR), were constructed. Rat BMVECs were seeded onto 24-well plates and cotransfected with 500 ng of pmiR-VEGF-wt or pmiR-VEGF-mut plasmids and 100 nM mimic negative control or miR-150 mimic by Lipofectamine 2000 for 48 h, cells were harvested, and then, the luciferase activity levels were quantified by a dual-luciferase reporter assay system (Promega, Beijing, China) according to manufacturer instructions. This assay was repeated six times.

Identification of Target mRNAs of miR-150

To determine the gene targets of miR-150, four leading miRNA target prediction algorithms (TargetScan 4.1, miRanda, miRbase, RNAhybrid) were used.

Western Blotting

According to our previously published protocols [4], Cells were harvested and lysed immediately. Total protein concentrations of samples were determined by protein assay kit (Bio-Rad, Hercules, CA, USA). Samples (30 μg/lane) were put into the lane of 10% SDS–polyacrylamide gels to electrophoresis and the proteins were separated and then transferred to polyvinylidene difluoride membranes. Membranes were cut into sections, and sections contained target proteins were immersed in skimmed milk (5%) for 1 h to block nonspecific binding sites and then incubated with the polyclonal rabbit anti-VEGF antibody (Abcam, 1:2000) or rabbit anti-β-actin antibody (Abcam, Cambridge, MA, USA, 1:2,000) overnight at 4°C, and then incubated 1 h with corresponding horseradish peroxidase conjugated secondary antibody (Sigma-Aldrich, St. Louis, MO, USA, 1:10,000). Immunoblots were visualized by a chemiluminescence kit (Thermo Scientific, Rockford, IL, USA), and repeated three times.

Capillary Density Measurement

According our previously published protocols [17], capillaries were identified by FITC-dextran (about 70,000 molecular weight, 0.2 mL/rat, Sigma-Aldrich, USA). Briefly, rats (n = 9–11/group) were intravenous injected FITC-dextran 10 min before sacrificed on the 7th day after MCAO. Three coronal cryosections of 20 μm

thick per rat at the same position (0.2, 0.8, and 2.8 mm posterior to bregma) were analyzed by a multiphoton scanning microscope (TCS SP5, Nikon, Japan). Ten visual fields of each section were taken in the infarct border zone (IBZ). All the digitized images were set the same threshold to ensure that FITC-dextran-perfused patterns were reflected by FITC pixels. Results were presented as fold changes of number of FITC pixels, and the control group was set to 1.

Statistical Analysis

Data were showed as mean ± standard deviation (SD). Statistical Package for the Social Sciences (SPSS 14.0, IBM, Armonk, NY, USA) software was used for statistical analysis. The one-way analysis of variance (ANOVA) of Fisher's least significant difference (LSD) test or two-tailed Student's *t*-test was used. $P < 0.05$ was considered significant.

Results

MiR-150 is Downregulated after Ischemia

To assess the expression of miR-150 after ischemia, rats were subjected to MCAO and miR-150 in the brain and blood was detected by RT-PCR. MiR-150 expression was found to decrease significantly in different experimental time following ischemia. MiR-150 expression in the brain was decreased to 20.7% ± 3.1% compared with the sham group on the 1st day after ischemia ($P < 0.05$), and further decreased to 10.6% ± 3.6% after 3rd day ($P < 0.05$), which was the lowest time point, and decreased to 33.4% ± 6.2% yet after the 7th day ($P < 0.05$) (Figure 1A). Data of miR-150 expression in the brain were normalized by those of the contralateral side, and miR-150 expression in the contralateral side of different groups had no statistical significant. MiR-150 expression in the blood also exhibited similar change after ischemia (Figure 1B). The miR-150 expression was decreased obviously after ischemia and downregulated mostly on the 3rd day after stroke (sham: 100% ± 21.3%, 1st day: 29.1% ± 2.8%, 3rd day: 10.6% ± 3.6%, 7th day: 23.4% ± 6.4%, $P < 0.05$), while the expression of VEGF protein in the IBZ was negatively related to the expression of miR-150 (Figure 1C–E). VEGF protein expression increased from the 1st day to the 7th day after ischemia (sham: 1 ± 0.06, 1st day: 1.52 ± 0.06, 3rd day: 1.99 ± 0.14, 7th day: 1.17 ± 0.05, $P < 0.05$). To assess expression changes of miR-150 after ischemia in cells of blood–brain barrier, BMVECs and astrocytes, the main component cells, were exposed to OGD for different time periods. Results showed that OGD significantly decreased the expression of miR-150 in BMVECs and astrocytes. Expression of miR-150 in BMVECs (control: 100% ± 5.0%, 2 h OGD: 46.4% ± 4.1%, 4 h OGD: 27.7% ± 2.9%, $P < 0.05$) and astrocytes (control: 100% ± 5.4%, 2 h OGD: 20.4% ± 4.1%, 4 h OGD: 27.1% ± 3.1%, $P < 0.05$) was decreased and was further decreased after 4 h OGD (Figure 1F–G), and miR-150 expression in BMVECs is much higher than in astrocytes (23.2 ± 2.1 vs.*1.0* ± 0.06, $P < 0.05$) (Figure 1H), while expression of VEGF proteins in BMVECs after 2 or 4 h OGD was increased (control: 1.0 ± 0.06, 2 h OGD: 1.49 ± 0.09, 4 h OGD: 2.35 ± 0.14, $P < 0.05$) (Figure 1I–J).

MiR-150 Controls Cerebral Angiogenesis after MCAO in Rats

We have found that the expression of miR-150 was decreased and was negatively related to VEGF expression after stroke, and thus, we speculate that the downregulation of miR-150 might promote angiogenesis after stroke. To confirm this hypothesis, we upregulated the miR-150 expression by miR-150 agomir and tested the function of miR-150 on angiogenesis *in vivo* according to published protocols [18]. Intracerebroventricular miR-150 agomir injected rats exhibited a significantly increased miR-150 expression in IBZ in comparison with the control groups measured by RT-PCR after 7 days MCAO (sham: 1.0 ± 0.13, MCAO: 0.33 ± 0.06, agomir control: 0.37 ± 0.05, agomir: 34.42 ± 5.47, $P < 0.05$) (Figure 2D). Vascular density of IBZ (sham: 1.0 ± 0.05, MCAO: 2.12 ± 0.18, agomir control: 1.85 ± 0.13 agomir: 0.46 ± 0.05, $P < 0.05$) (Figure 2E–F) and the expression of VEGF protein (sham: 1.0 ± 0.06, MCAO: 1.70 ± 0.13, agomir control: 1.72 ± 0.16 agomir: 0.57 ± 0.06, $P < 0.05$) (Figure 2B–C) were significantly reversed by miR-150 agomir treatment on the 7th day after MCAO.

MiR-150 Regulates BMVECs Capillary-like Tube Formation

To further confirm the function of miR-150 on angiogenesis, the capability of BMVECs in capillary-like tube formation was tested as previously reported [19]. Results showed that miR-150 mimic decreased the length of capillary-like structures significantly in normal condition (5.41 ± 0.27 vs. 2.98 ± 0.15 mm/mm^2, $P < 0.05$) and in OGD condition (6.56 ± 0.34 vs. 4.32 ± 0.23 mm/mm^2, $P < 0.05$) (Figure 3A–B), while miR-150 inhibitor increased the length of capillary-like structures significantly in normal condition (5.02 ± 0.25 vs. 7.28 ± 0.36 mm/mm^2, $P < 0.05$) and in OGD condition (6.38 ± 0.48 vs. 9.74 ± 0.59 mm/mm^2, $P < 0.05$) (Figure 3C–D).

MiR-150 Regulates BMVECs Proliferation and Migration

As the proliferation and migration of BMVECs are the key processes involved in cerebral angiogenesis, we also assessed whether miR-150 mediated proliferation and migration by immunofluorescence and scratch test, respectively. Results showed that miR-150 inhibited the proliferation of BMVECs. MiR-150 over-expression decreased the number of Ki-67-positive staining BMVECs significantly in normal condition (32.4% ± 4.5% vs. 4.9% ± 0.7%, $P < 0.05$) and in OGD condition (43.2% ± 5.1% vs. 11.5% ± 2.4%, $P < 0.05$) (Figure 4A–B), while miR-150 downregulation increased the number of Ki-67-positive staining BMVECs in normal condition (31.5% ± 4.7% vs. 56.5% ± 8.5%, $P < 0.05$) and in OGD condition (40.9% ± 5.4% vs. 74.5% ± 5.6%, $P < 0.05$) (Figure 4C–D).

MiR-150 also inhibited BMVECs migration, we found that miR-150 over-expression significantly decreased the migration distance of BMVECs in normal condition (100% ± 16.1% vs. 70.6% ± 5.5%, $P < 0.05$) and in OGD condition (121.5% ± 12.9% vs. 85.1% ± 10.2%, $P < 0.05$) (Figure 3E–F), while miR-150

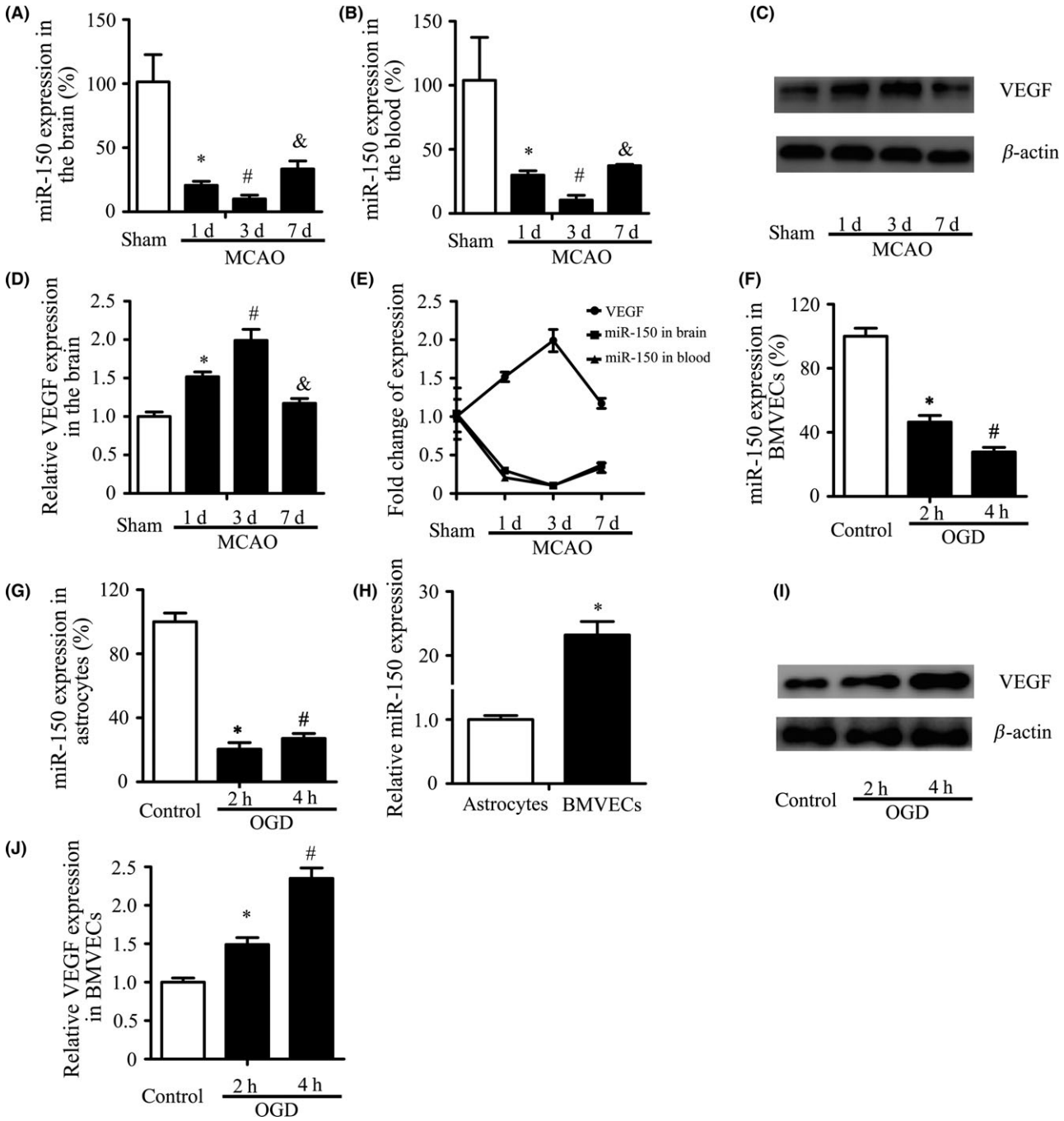

Figure 1 MiR-150 is Downregulated after Ischemia. (**A**–**B**) MiR-150 expression decreased significantly following ischemia in brain and blood. Sprague Dawley rats were randomly assigned to four groups (sham, 1, 3, 7 days after MCAO), n = 5. U6 and miR-16 were used as the internal control, respectively, and data of miR-150 expression in the brain were normalized by those of the contralateral side. Data were related to the sham group and showed as mean ± standard deviation (SD). $^{*}P < 0.05$ vs. the sham control, $^{\#}P < 0.05$ vs. 1 day, $^{\&}P < 0.05$ vs. 3 day. (**C**–**E**) The expression of VEGF protein in the ischemic border zone (IBZ) was increased following ischemia and negatively related to miR-150. β-Actin was used as the internal control. Data were related to the sham group and showed as mean ± standard deviation (SD). $^{*}P < 0.05$ vs. the sham control, $^{\#}P < 0.05$ vs. 1 day, $^{\&}P < 0.05$ vs. 3 day. (**F**–**G**) The expression of miR-150 in BMVECs and astrocytes decreased significantly. Brain microvascular endothelial cells (BMVECs) and astrocytes were treated with oxygen–glucose deprivation (OGD) for 2, 4 h. U6 was used as the internal control. $^{*}P < 0.05$ vs. the control, $^{\#}P < 0.05$ vs.2 h. (**H**) MiR-150 expression in BMVECs was much higher than in astrocytes. U6 was used as the internal control. $^{*}P < 0.05$. (**I**–**J**) The expression of VEGF protein in BMVECs was increased significantly after OGD. β-Actin was used as the internal control. $^{*}P < 0.05$ vs. the control, $^{\#}P < 0.05$ vs. 2 h.

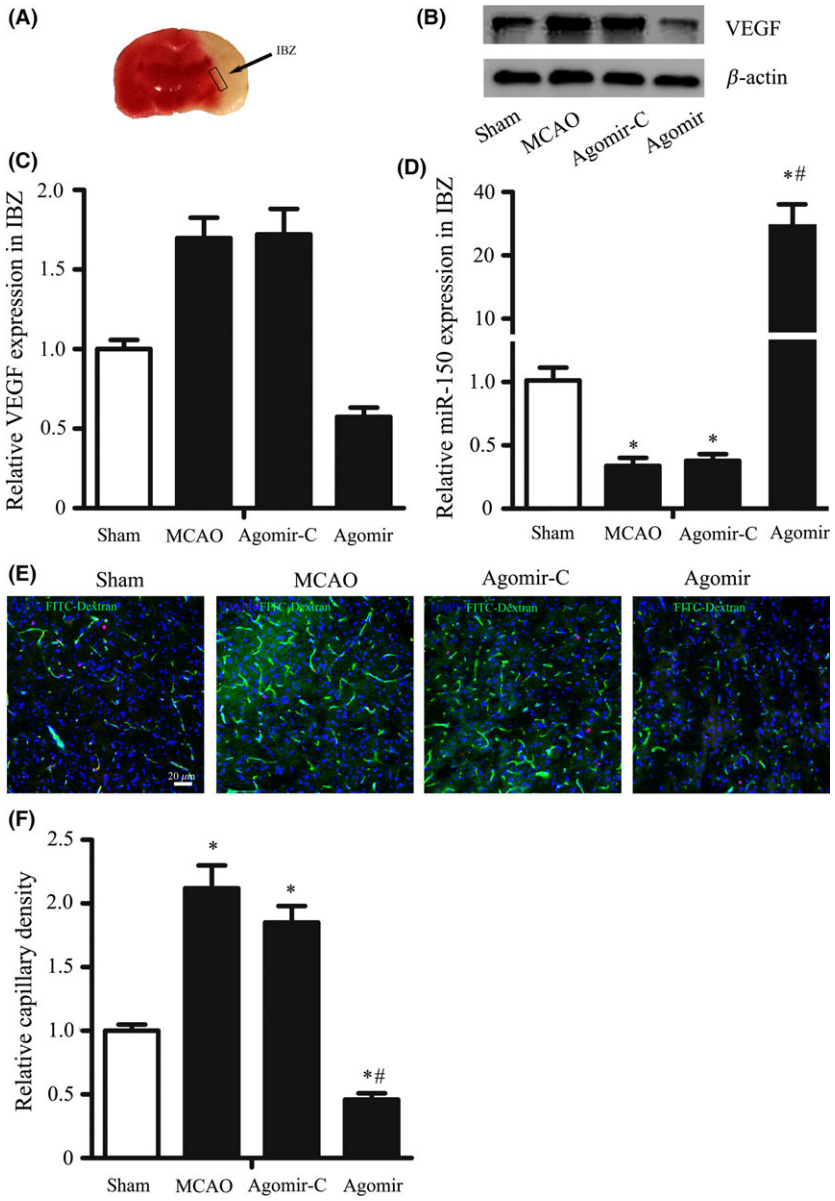

Figure 2 MiR-150 Controls Cerebral Angiogenesis after MCAO in Rats. Rats were randomly assigned to 4 groups: sham, n = 8, MCAO, n = 6, agomir control (agomir-C), n = 7, and miR-150 agomir, n = 5. (**A**) Representative IBZ was showed, where the brain sample was obtained on the 7th following MCAO. (**B**-**C**) MiR-150 agomir reversed the increase of VEGF protein expression in the IBZ following MCAO. β-Actin was used as the internal control.*$P < 0.05$, vs. sham group, # $P < 0.05$ vs. agomir control group. (**D**) MiR-150 agomir increased the expression of miR-150 in IBZ after MCAO. MiR-150 was detected by RT-PCR, and U6 was used as the internal control. (**E**–**F**) MiR-150 agomir reversed the increase of capillary density in IBZ following MCAO. (**E**) The representative pictures of immunofluorescence staining of frozen sections taken from the IBZ were shown (blue for DAPI, pink for Ki-67, and green for FITC-dextran, FITC). Bar = 20 μm. 2F the results showed that capillary density in IBZ was significantly increased after MCAO, while miR-150 agomir reversed this change after MCAO. *$P < 0.05$ vs. sham groups, # $P < 0.05$ vs. agomir control group.

downregulation significantly increased the migration distance of BMVECs normal condition (100% ± 16.3% vs. 135.5% ± 10.3%, $P < 0.05$) and in OGD condition (128.6% ± 17.2% vs. 165.3% ± 11.7%, $P < 0.05$) (Figure 4G–H).

MiR-150 Directly Regulates the Expression of VEGF

We analyzed putative miR-150 targets predicted by defined criteria using four target prediction software programs (TargetScan 4.1, miRanda, miRbase, and RNAhybrid). The predicted targets VEGF, which can regulate endothelial cell functions and vessel growth, were picked out (Figure 5C) and confirmed by Western blot. The results showed that miR-150 over-expression significantly decreased the expression of VEGF protein (1.0 ± 0.06 vs. 0.38 ± 0.06, $P < 0.05$), while miR-150 downregulation significantly increased the expression of VEGF protein (1.0 ± 0.07 vs. 1.52 ± 0.13, $P < 0.05$) (Figure 5A–B). Furthermore, with dual-luciferase assay, VEGF was recognized as the direct target of miR-150 (Figure 5D).

VEGF Mediated the Increase of BMVECs Capillary-like Tube Formation, Proliferation, and Migration by MiR-150 Inhibitor

To confirm the function of VEGF in miR-150-mediated cerebral angiogenesis, we used VEGF-neutralizing antibody to inhibit its function. Results showed that VEGF-neutralizing antibody significantly reversed miR-150 downregulation induced increase of capillary-like tube formation (7.19 ± 0.74 vs. 4.03 ± 0.46 mm/

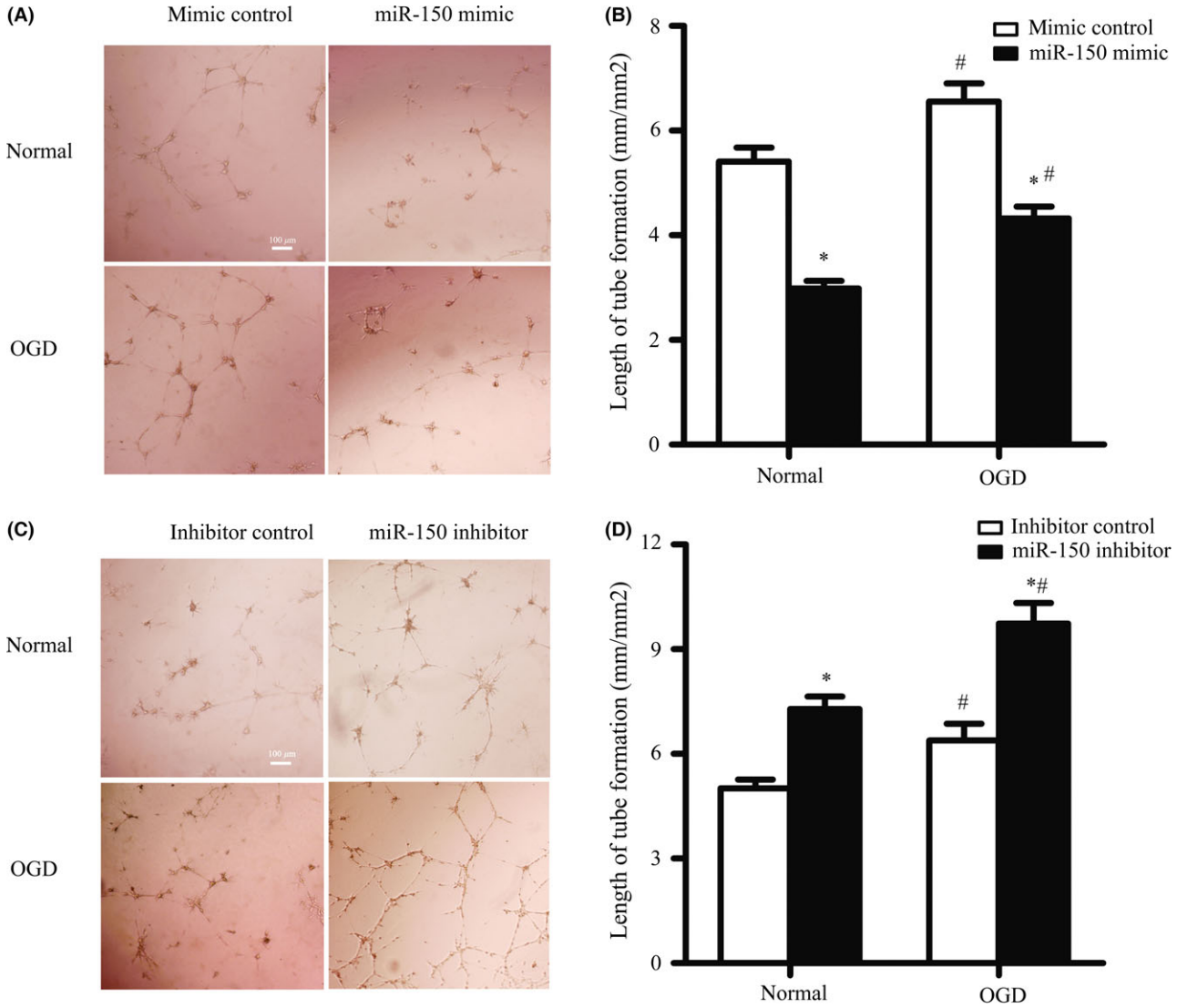

Figure 3 MiR-150 Regulates BMVECs Capillary-like Tube Formation. (**A**–**B**) miR-150 mimic inhibited the capillary-like tube formation in brain microvascular endothelial cells (BMVECs) in normal condition and oxygen–glucose deprivation (OGD) condition. BMVECs were transfected by miR-150 mimic or mimic control, and the length of capillary-like tube structure was measured. Bar = 100 μm. *$P < 0.05$ vs. the control group, $^{\#}P < 0.05$ vs. the normal group. (**C**–**D**) MiR-150 inhibitor promoted the capillary-like tube formation in BMVECs in normal condition and OGD condition. BMVECs were transfected by miR-150 mimic or mimic control, and the length of capillary-like tube structure was measured. Bar = 100 μm. *$P < 0.05$ vs. the control group, $^{\#}P < 0.05$ vs. the normal group.

mm^2, $P < 0.05$), cell proliferation (73.2% ± 9.1% vs. 55.0% ± 6.7%, $P < 0.05$), and cell migration (136.7% ± 14.3% vs. 63.7% ± 5.4%, $P < 0.05$) (Figure 6A–F).

Discussion and Conclusion

This study showed that 1. the expression of miR-150 decreased significantly in brain and serum of rats subjected to cerebral ischemia, and in oxygen–glucose-deprived BMVECs and astrocytes, which is negatively related to the expression of VEGF protein in BMVECs. 2. miR-150 upregulation suppressed proliferation, migration, tube formation in BMVECs and decreased the vascular density of IBZ, while miR-150 downregulation promoted proliferation, migration, tube formation in BMVECs. 3. miR-150 regulates VEGF expression and VEGF is the direct target of miR-150 confirmed by dual-luciferase assay. 4. miR-150 regulates BMVECs proliferation, migration, tube formation via VEGF.

According to the previous studies, ischemia or OGD could result in changes in miRNA expression [20–24]. Increasing evidences show that hypoxia regulates the expression of miRNAs by hypoxia-inducible factor-dependent (HIF) mechanisms [25]. However, it is noteworthy that stroke is an involved pathological process and it is difficult to attribute any change of miRNAs to a single

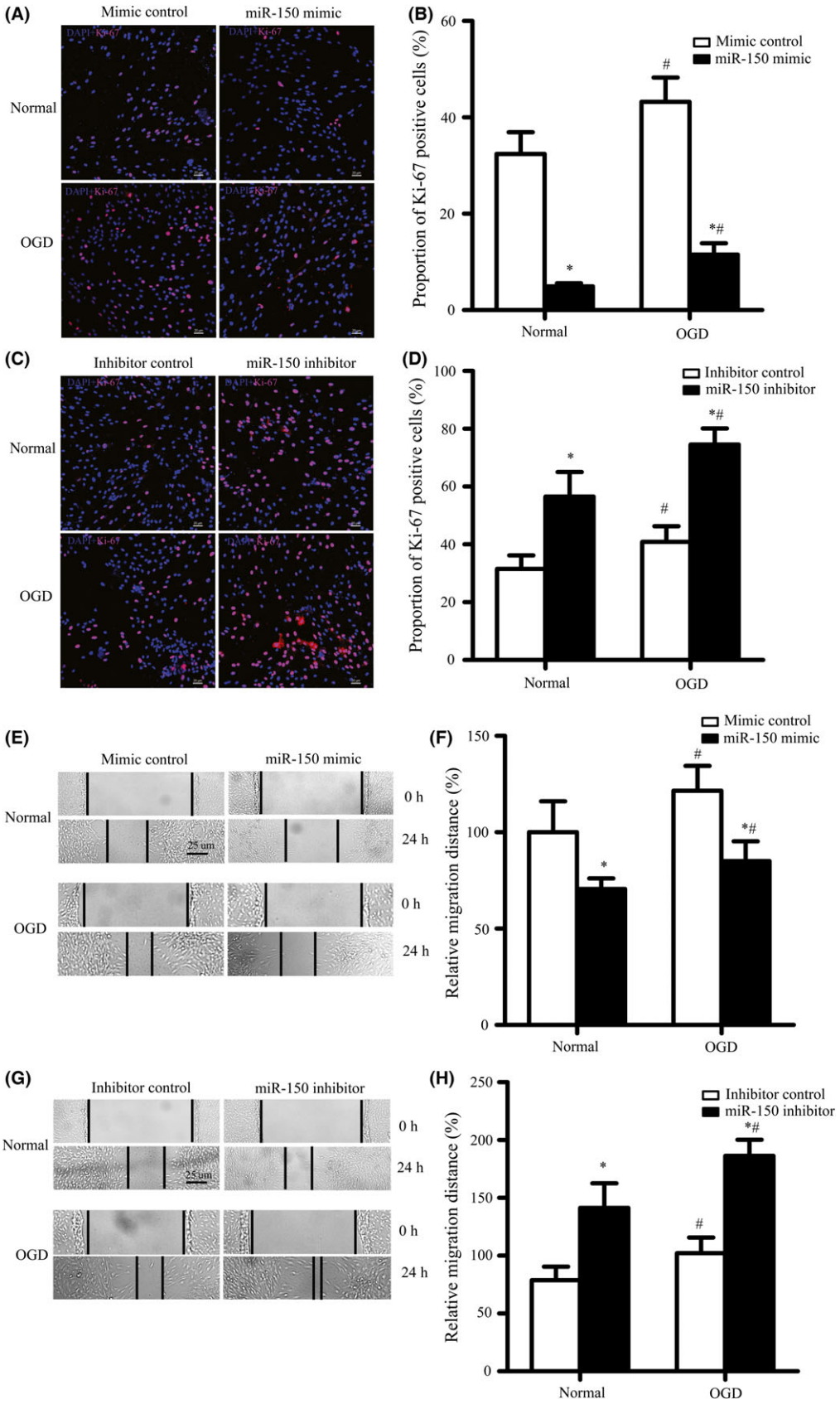

Figure 4 MiR-150 Regulates BMVECs Proliferation and Migration. (**A**–**D**) MiR-150 mimic decreased the proportion of Ki-67-positive staining BMVECs in normal condition and oxygen–glucose deprivation (OGD) condition (**A**–**B**), while miR-150 inhibitor increased the proportion of Ki-67-positive staining BMVECs in normal condition and OGD condition (4**C**–**D**). *$P < 0.05$ vs. the control group, #$P < 0.05$ vs. the normal group. The representative pictures of immunofluorescence (pink for Ki-67, blue for DAPI) were shown. Bar = 20 μm. *$P < 0.05$ vs. the control group. (**E**–**H**) MiR-150 mimic decreased the distance of BMVECs migration in normal condition and OGD condition (4E-F), while miR-150 inhibitor increased it. (**G**–**H**) The representative pictures of the scratch tests were captured and the distance of migration was quantified. Bar = 25 μm. *$P < 0.05$ vs. the control group, #$P < 0.05$ vs. the normal group.

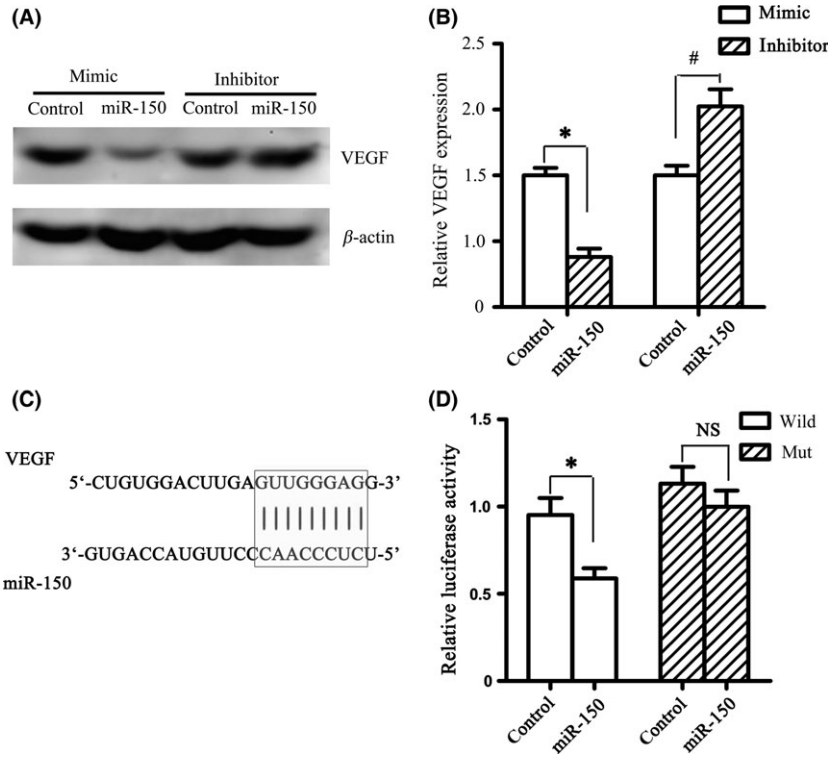

Figure 5 MiR-150 Directly Regulates the Expression of VEGF. (**A**–**B**) MiR-150 mimic decreased VEGF protein expression in BMVECs, while miR-150 inhibitor increased VEGF protein expression. The protein expression of VEGF after 24-h transfection was detected by Western blot. *$P < 0.05$ vs. mimic control group, #$P < 0.05$ vs. inhibitor control group. (**C**) Bioinformatic analysis showed that complementary regions were identified in the 3′-UTR of VEGF. (**D**) By dual-luciferase assay, VEGF was recognized as the direct target of miR-150. The ratio of luciferase activity of each type was calculated either in the presence or absence of exogenous miR-150. *$P < 0.05$ vs. control group in cotransfected with pmiR-VEGF-wt, while no significant difference (NS) in cotransfected with pmiR-VEGF-mut.

pathogenic factor. Thus, more research is needed to explore the factors that regulate the change of miR-150 expression after stroke. Moreover, miR-150 was found to be expressed in some other cells, such as monocytes [26], platelets [27, 28], tumor cells [29, 30], but we mainly detected the miR-150 changes in BMVECs and astrocytes, which constitutes the first-line interface with blood to detect changes in oxygen level after stroke [31]. We found miR-150 expression in both cells was decreased significantly after OGD. Of note, a bit increase of miR-150 expression in astrocytes after 4 h OGD than after 2 h OGD might due to the ischemic tolerance of astrocytes, but more research is needed to verify it. Furthermore, changes in the circulating level of miR-150 indicate that miR-150 might serve as a potential novel biomarker of ischemic stroke.

The discovery of miRNAs can silence target genes post-transcriptionally shed light on exploring the function of noncoding RNAs in angiogenesis. The initial evidences have shown the importance of miRNAs in the regulation of angiogenesis arose from several experiments about Dicer, the key RNAse of the miRNAs synthesis, with a genetic manipulation [32, 33]. Now a number of studies have demonstrated that miRNAs could regulate angiogenesis and even the term "angiomiR" has been coined to emphasize the function [34].

Although miR-150 is believed to be involved in angiogenesis, its role in the regulation of angiogenesis remains controversial. There were a series of studies that alluded miR-150 as a cancer suppressor which inhibited cancer metastasis and angiogenesis by targeting c-Myb [35, 36]. Moreover, Shen et al. [14] reported that miR-150, as an anti-angiomiR, inhibits retinal angiogenesis by targeting PDGF and Notch4 in a model of oxygen-induced ischemic retinopathy in mouse. Furthermore, miR-150 could inhibit the migration of human bone marrow-derived mononuclear cells and endothelial progenitor cells (EPCs) by targeting CXCR4 [37, 38]. Our study was in accord with the former researches and found that miR-150 suppressed BMVECs angiogenesis in normal condition *in vitro* and over-expression of miR-150 could deteriorate cerebral angiogenesis in a rat MCAO model. However, this view recently is challenged by Zhang and his colleagues (2013), showing that microvesicles shed from the monocytic cell line THP-1 were enriched with miR-150 which could promote angiogenesis by suppressing the migration by targeting c-Myb [26] and miR-150 from tumor-associated

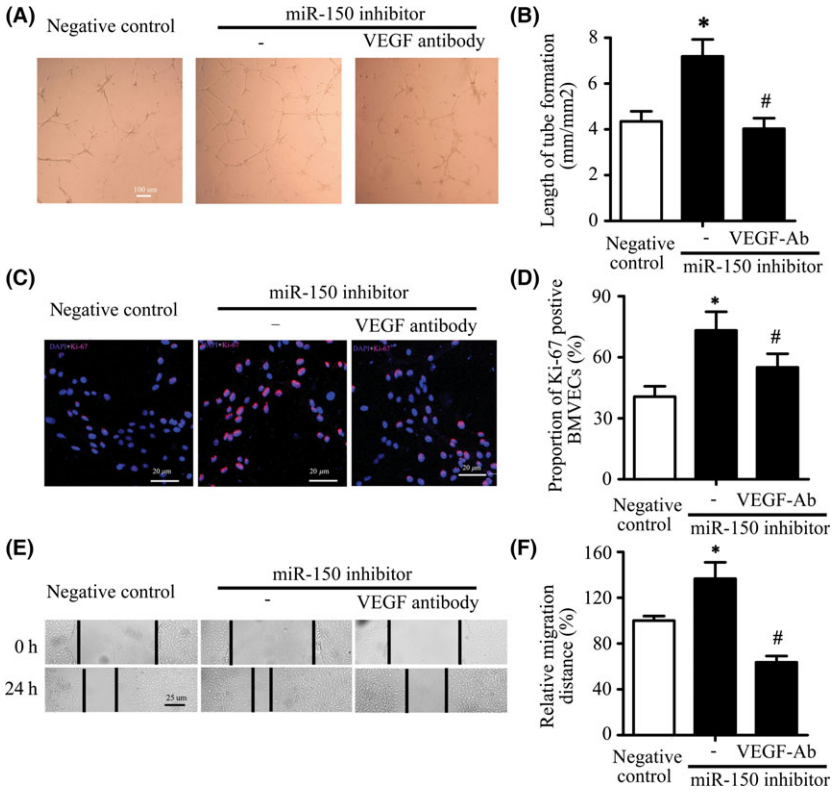

Figure 6 VEGF Mediated the Increase of BMVECs Capillary-like Tube Formation, Proliferation, and Migration by MiR-150 Inhibitor. (**A**–**B**) VEGF-neutralizing antibody significantly reversed miR-150 downregulation induced increase of capillary-like tube formation. The representative pictures of tube formation were shown, and the length of tube formation was measured. Bar = 100 μm. *P < 0.05 vs. the inhibitor control group, $^{\#}P$ < 0.05 vs. the miR-150 inhibitor. (**C**–**D**) VEGF-neutralizing antibody significantly reversed miR-150 downregulation induced increase of Ki-67-positive staining proportion of BMVECs. Pink for Ki-67, blue for DAPI, Bar = 20 μm. *P < 0.05 vs. the inhibitor control group, $^{\#}P$ < 0.05 vs. the miR-150 inhibitor. (**E**–**F**) VEGF-neutralizing antibody significantly reversed miR-150 downregulation induced increase of migration distance of BMVECs. Bar = 25 μm. *P < 0.05 vs. the inhibitor control group, $^{\#}P$ < 0.05 vs. the miR-150 inhibitor.

macrophages derived microvesicles could upregulation VEGF to attenuate tumor development [15]. This discrepancy may result from different pathological conditions and the different miR-150 sources, the microvesicles. Of note, the microvesicle-delivery miR-150 may upregulate VEGF with an indirect manner, because miRNAs are a noncoding RNA which usually can silence the direct targeting genes and one miRNA could regulate dozens, even hundreds of targets. However, according to our study, VEGF may be the direct target of miR-150 in BMVECs after stroke. This expands new knowledge on post-transcriptional regulation about VEGF. As VEGF own the dual function in vascular biology: the induction of blood-brain barrier (BBB) disruption and the regulation of angiogenesis, miR-150 can also affect the permeability of BBB and angiogenesis. In fact, the vascular splitting is a important step for angiogenesis at the beginning[39]. After stroke, delayed treatment with VEGF can promote angiogenesis and recovery[40], while blocking VEGF also may improve the recovery by protecting BBB from broking down[41]. Thus, appropriate amount of VEGF at the right time is needed for stroke recovery.

Nevertheless, there is still possible that indirect mechanisms may increase the potency of miR-150 action on VEGF. Several studies have reported miR-150 also could directly regulate some other angiogenic factors (for instance, Notch3) or indirectly regulate by nuclear transcription factors (for instance, HIF-1a) [42, 43]. Thus, miR-150 might directly regulate VEGF at the first beginning, and the indirect regulation may also work lately. Of note, one main hurdle that has limited the interpretation of many miRNA profiling studies is the difficulty of identifying all the miRNA targets. Furthermore, miRNAs can interact with each other. One miRNA may promote or inhibit another miRNA by the principle of complementary base pairing. Thus, the role of miR-150 in poststroke angiogenesis is quite complicated and more studies may be necessary.

Besides angiogenesis, miR-150 may also play an important role in some other pathophysiological courses. It was reported that miR-150 was involved in high glucose-induced hypertrophy of cardiomyocytes [44] and renal mesangial cells aging [45]. Finally, we have to admit that the use of young rats in this study to decrease the mortality rate may have some limitation because nearly three-quarters of all strokes occur in people over the age of 65.

Taken together, we have demonstrated that miR-150 directly targeting VEGF could serve as an anti-angiomiR of BMVECs in poststroke angiogenesis. Thus, miR-150 is an epigenetic regulator of VEGF, and miR-150 may be a potential novel therapeutic target for stroke treatment.

Conflict of Interest

The authors declare no conflict of interest.

Acknowledgments

This work was supported by National Natural Science Foundation of China (Grants: 81571119 and 81371311 to BH, 81400969 to QWH, 81571139 to LM, 81301165 to JHJ, and 81301002 to YPX).

References

1. Ferrara N, Kerbel RS. Angiogenesis as a therapeutic target. *Nature* 2005;**438**:967–974.
2. Wang J, Shi Y, Zhang L, et al. Omega-3 polyunsaturated fatty acids enhance cerebral angiogenesis and provide long-term protection after stroke. *Neurobiol Dis* 2014;**68**:91–103.
3. Giacca M, Zacchigna S. VEGF gene therapy: therapeutic angiogenesis in the clinic and beyond. *Gene Ther* 2012;**19**:622–629.
4. He QW, Xia YP, Chen SC, et al. Astrocyte-derived sonic hedgehog contributes to angiogenesis in brain microvascular endothelial cells via RhoA/ROCK pathway after oxygen-glucose deprivation. *Mol Neurobiol* 2013;**47**:976–987.
5. Xia YP, He QW, Li YN, et al. Recombinant human sonic hedgehog protein regulates the expression of ZO-1 and occludin by activating angiopoietin-1 in stroke damage. *PLoS One* 2013;**8**:e68891.
6. Li Y, Xia Y, Wang Y, et al. Sonic hedgehog (Shh) regulates the expression of angiogenic growth factors in oxygen-glucose-deprived astrocytes by mediating the nuclear receptor NR2F2. *Mol Neurobiol* 2013;**47**:967–975.
7. Pola R, Ling LE, Silver M, et al. The morphogen Sonic hedgehog is an indirect angiogenic agent upregulating two families of angiogenic growth factors. *Nat Med* 2001;**7**:706–711.
8. Ghorpade DS, Holla S, Kaveri SV, Bayry J, Patil SA, Balaji KN. Sonic hedgehog-dependent induction of microRNA 31 and microRNA 150 regulates Mycobacterium bovis BCG-driven toll-like receptor 2 signaling. *Mol Cell Biol* 2013;**33**:543–556.
9. Fayyad-Kazan H, Bitar N, Najar M, et al. Circulating miR-150 and miR-342 in plasma are novel potential biomarkers for acute myeloid leukemia. *J Transl Med* 2013;**11**:31.
10. Ito M, Teshima K, Ikeda S, et al. MicroRNA-150 inhibits tumor invasion and metastasis by targeting the chemokine receptor CCR6, in advanced cutaneous T-cell lymphoma. *Blood* 2014;**123**:1499–1511.
11. Mraz M, Kipps TJ. MicroRNAs and B cell receptor signaling in chronic lymphocytic leukemia. *Leuk Lymphoma* 2013;**54**:1836–1839.
12. Srivastava SK, Bhardwaj A, Singh S, et al. MicroRNA-150 directly targets MUC4 and suppresses growth and malignant behavior of pancreatic cancer cells. *Carcinogenesis* 2011;**32**:1832–1839.
13. Luo Z, Wen G, Wang G, et al. MicroRNA-200C and -150 play an important role in endothelial cell differentiation and vasculogenesis by targeting transcription repressor ZEB1. *Stem Cells* 2013;**31**:1749–1762.
14. Shen J, Yang X, Xie B, et al. MicroRNAs regulate ocular neovascularization. *Mol Ther* 2008;**16**:1208–1216.
15. Liu Y, Zhao L, Li D, et al. Microvesicle-delivery miR-150 promotes tumorigenesis by up-regulating VEGF, and the neutralization of miR-150 attenuate tumor development. *Protein Cell* 2013;**4**:932–941.
16. Liu CH, Sun Y, Li J, et al. Endothelial microRNA-150 is an intrinsic suppressor of pathologic ocular neovascularization. *Proc Natl Acad Sci U S A* 2015;**112**:12163–12168.
17. Mao L, Huang M, Chen SC, et al. Endogenous endothelial progenitor cells participate in neovascularization via CXCR4/SDF-1 axis and improve outcome after stroke. *CNS Neurosci Ther* 2014;**20**:460–468.
18. Wang X, Guo B, Li Q, et al. miR-214 targets ATF4 to inhibit bone formation. *Nat Med* 2013;**19**:93–100.
19. Presneau N, Eskandarpour M, Shemais T, et al. MicroRNA profiling of peripheral nerve sheath tumours identifies miR-29c as a tumour suppressor gene involved in tumour progression. *Br J Cancer* 2013;**108**:964–972.
20. Zhang J, Ren J, Chen H, Geng Q. Inflammation induced-endothelial cells release angiogenesis associated-microRNAs into circulation by microparticles. *Chin Med J (Engl)* 2014;**127**:2212–2217.
21. Moon JM, Xu L, Giffard RG. Inhibition of microRNA-181 reduces forebrain ischemia-induced neuronal loss. *J Cereb Blood Flow Metab* 2013;**33**:1976–1982.
22. Ouyang YB, Stary CM, Yang GY, Giffard R. MicroRNAs: innovative targets for cerebral ischemia and stroke. *Curr Drug Targets* 2013;**14**:90–101.
23. Zeng L, Liu J, Wang Y, et al. MicroRNA-210 as a novel blood biomarker in acute cerebral ischemia. *Front Biosci (Elite Ed)* 2011;**3**:1265–1272.
24. Sun Y, Gui H, Li Q, et al. MicroRNA-124 protects neurons against apoptosis in cerebral ischemic stroke. *CNS Neurosci Ther* 2013;**19**:813–819.
25. Lendahl U, Lee KL, Yang H, Poellinger L. Generating specificity and diversity in the transcriptional response to hypoxia. *Nat Rev Genet* 2009;**10**:821–832.
26. Li J, Zhang Y, Liu Y, et al. Microvesicle-mediated transfer of microRNA-150 from monocytes to endothelial cells promotes angiogenesis. *J Biol Chem* 2013;**288**:23586–23596.
27. Goren Y, Meiri E, Hogan C, et al. Relation of reduced expression of MiR-150 in platelets to atrial fibrillation in patients with chronic systolic heart failure. *Am J Cardiol* 2014;**113**:976–981.
28. Edelstein LC, McKenzie SE, Shaw C, Holinstat MA, Kunapuli SP, Bray PF. MicroRNAs in platelet production and activation. *J Thromb Haemost* 2013;**11**(Suppl 1):340–350.
29. Cao M, Hou D, Liang H, et al. miR-150 promotes the proliferation and migration of lung cancer cells by targeting SRC kinase signalling inhibitor 1. *Eur J Cancer* 2014;**50**:1013–1024.
30. Ma Y, Zhang P, Wang F, et al. miR-150 as a potential biomarker associated with prognosis and therapeutic outcome in colorectal cancer. *Gut* 2012;**61**:1447–1453.
31. Weiss N, Miller F, Cazaubon S, Couraud PO. The blood-brain barrier in brain homeostasis and neurological diseases. *Biochim Biophys Acta* 2009;**1788**:842–857.
32. Chen Z, Lai TC, Jan YH, et al. Hypoxia-responsive miRNAs target argonaute 1 to promote angiogenesis. *J Clin Invest* 2013;**123**:1057–1067.
33. Meloni M, Marchetti M, Garner K, et al. Local inhibition of microRNA-24 improves reparative angiogenesis and left ventricle remodeling and function in mice with myocardial infarction. *Mol Ther* 2013;**21**:1390–1402.
34. Wang SS, Olson EN. AngiomiRs-Key regulators of angiogenesis. *Curr Opin Genet Dev* 2009;**19**:205–211.
35. Persson M, Andren Y, Mark J, Horlings HM, Persson F, Stenman G. Recurrent fusion of MYB and NFIB transcription factor genes in carcinomas of the breast and head and neck. *Proc Natl Acad Sci U S A* 2009;**106**:18740–18744.
36. Jiang X, Huang H, Li Z, et al. Blockade of miR-150 maturation by MLL-fusion/MYC/LIN-28 is required for MLL-associated leukemia. *Cancer Cell* 2012;**22**:524–535.
37. Rolland-Turner M, Goretti E, Bousquenaud M, et al. Adenosine stimulates the migration of human endothelial progenitor cells. Role of CXCR4 and microRNA-150. *PLoS One* 2013;**8**:e54135.
38. Tano N, Kim HW, Ashraf M. microRNA-150 regulates mobilization and migration of bone marrow-derived mononuclear cells by targeting Cxcr4. *PLoS One* 2011;**6**:e23114.
39. Makanya AN, Hlushchuk R, Djonov VG. Intussusceptive angiogenesis and its role in vascular morphogenesis, patterning, and remodeling. *Angiogenesis* 2009;**12**:113–123.
40. Dzietko M, Derugin N, Wendland MF, Vexler ZS, Ferriero DM. Delayed VEGF treatment enhances angiogenesis and recovery after neonatal focal rodent stroke. *Transl Stroke Res* 2013;**4**:189–200.
41. Reeson P, Tennant KA, Gerrow K, et al. Delayed inhibition of VEGF signaling after stroke attenuates blood-brain barrier breakdown and improves functional recovery in a comorbidity-dependent manner. *J Neurosci* 2015;**35**:5128–5143.
42. Ghisi M, Corradin A, Basso K, et al. Modulation of microRNA expression in human T-cell development: targeting of NOTCH3 by miR-150. *Blood* 2011;**117**:7053–7062.
43. Yu ZY, Bai YN, Luo LX, Wu H, Zeng Y. Expression of microRNA-150 targeting vascular endothelial growth factor-A is downregulated under hypoxia during liver regeneration. *Mol Med Rep* 2013;**8**:287–293.
44. Duan Y, Zhou B, Su H, Liu Y, Du C. miR-150 regulates high glucose-induced cardiomyocyte hypertrophy by targeting the transcriptional co-activator p300. *Exp Cell Res* 2013;**319**:173–184.
45. Liu X, Fu B, Chen D, et al. miR-184 and miR-150 promote renal glomerular mesangial cell aging by targeting Rab1a and Rab31. *Exp Cell Res* 2015;**336**:192–203.